Journal Homepage: - www.journalijar.com

INTERNATIONAL JOURNAL OF ADVANCED RESEARCH (IJAR)

Article DOI: 10.21474/IJAR01/21410
DOI URL: http://dx.doi.org/10.21474/IJAR01/21410

ISSN NO. 2320-5407

RESEARCH ARTICLE

REALIZATION OF A SOLAR DRYER INDIRECT FOR THE KINETIC STUDY AND THERMODYNAMIC PROPERTIES OF MORINGA OLEIFERA LEAVES.

Codjo Goudjinou[1, 2], Michel Tchiekre[3], Wiwegnon Uriel-Longin Aguemon[4], Kowiou Aboudou[1], Sibiath G. Osseni[1], Berleo Apovo [2] , Mohamed M. Soumanou[1] and Clement Ahouannou[2]

1. Units of Research in Enzyme Engineering and Food (URGEA), Laboratory of tudy and
Applied Chemistry Research (LERCA), Department of Food Technology Engineering, High Polytechnic of Abomey-Calavi, Abomey-Calavi University, 01P.O.BOX 2009, Cotonou, Benin.
2. Laboratory of Energetic and Mechanic Applied (LEMA), High Polytechnic of Abomey-Calavi, Abomey-Calavi University, 01 P.O. BOX 2009, Cotonou, Benin.
3. Department of Mathematics physic Chemistry UPR Mathematics, University peleforo Gon Coulibaly of Korhogo.
4. Faculty of Sciences, Department of Mathematics, University of Kindia, Guinea.

Manuscript Info

Manuscript History
Received: 16 May 2025
Final Accepted: 19 June 2025
Published: July 2025

Key words:-
Solar dryer,Moringa oleifera,Drying kinetics,thermodynamic properties.

Abstract

In this article, we first presented the steps followed in the conception and realization of an indirect solar dryer in the Applied Energy and Me chanics laboratory (LEMA) of the Polytechnic School of Abomey-Calavi. Afterwards, we studied the thermal performance of the device and the influence of various drying conditions (temperature, relative humidity and air flow) on the drying process and the effective diffusivity of Moringa oleifera (Lam) leaves. The results show that the dryer recorded moderate temperature values varying between 38°C and 55°C over the entire test period. The relative humidity of the drying air present an evolution inversely proportional to that of the ambient air. The drying curves obtained currently, only a single period at decreasing speed (phase 2). In this period, the transfer of humidity between the air and the product was evaluated by applying the diffusive Fick model. The effective diffusivity varied from $8.456\ 10^{11}$ to $8.9567\ 10^{8}$ m^2s^1 with an increase in drying temperature and hot air flow rate. The Arrhe nius relationship expressing the effect of temperature on the effective diffusion coefficient gives an average activation energy value of 86.462 KJ/mol ±1.98. The drying speed is determined empirically from the Drying Characteristic Curve (CCS). Among the five models developed, Midilli and al. (2002) adequately describes the drying kinetics of *Moringa oleifera* leaves under the experimental conditions imposed.

Corresponding Author:- Codjo Goudjinou
Address:- 1. Units of Research in Enzyme Engineering and Food (URGEA), Laboratory of Study and Applied Chemistry Research (LERCA), Department of Food Technology Engineering, High Polytechnic of Abomey-Calavi, Abomey-Calavi University, 01P.O.BOX 2009, Cotonou, Benin.
2. Laboratory of Energetic and Mechanic Applied (LEMA), High Polytechnic of Abomey-Calavi, Abomey-Calavi University, 01 P.O. BOX 2009, Cotonou, Benin.

Introduction

The conservation of agricultural products is an essential imperative in developing countries where production is concentrated on short harvest periods. Thus, the development of post-harvest conservation and processing techniques for agricultural products in these countries becomes imperative in reducing the losses observed between harvest and the availability of the products on the market. In Africa, these losses are estimated on average at 25% for cereals and more than 50% for fruits, vegetables and tubers (Brito et al, 2021; FAO, 2023). Indeed, the enormous quantities of production, both agricultural (cereals, vegetables, fruits) and livestock (meat, fish, etc.), undergo various alterations following the lack of appropriate conservation and processing technologies. This leads to food shortages at certain times of the year and seriously affects the house hold economy. Thus, access of small farmers to effective post-harvest conservation techniques therefore becomes a development priority (Goudjinou, 2018; N'guessan, 2023). Among the different conservation techniques developed for agricultural products, drying remains the process most practiced by producers (Goudjinou et al., 2017; Ghenbazi; 2023). Indeed, in the agri-food sector, numerous research studies have been carried out to optimize the drying operation (Dissa et al., 2016, Goudjinou, 2018; Ghenbazi, 2023).

This operation consists of rationalizing both energy consumption and safe guarding the biological quality of the finished product. Nowadays, drying methods have diversified tanks to scientific and technological progress. Despite transfers of efficient technologies from the West, drying problems are numerous and do not seem to be resolved. Various failures indicate that developing countries must be offered more adapted technologies that take into account the real needs of the populations concerned (Ahouannou, 2001 ; Koua et al 2018 ; Ahouannou et al, 2023 ; Moctar et al, 2024). According to Masmoudi et al. (2008); Boubekri et al. (2009), solar drying constitutes an adequate solution for countries poor in conventional energy resources and with significant solar resources throughout the year. In this work, we realized an indirect solar dryer in order to understand the diffusional mechanisms that influence the drying process of Moringa leaves under controlled temperature and air flow conditions. The different tests consist of studying the separate influence of the various conditions of the drying air (temperature, relative humidity, air flow) on the drying process. The drying speed is determined empirically from the drying characteristic curve (CCS). Five (5) mathematical models existing in the literature were used for optimal adjustment of the experimental curves. This allowed us to determine the effective diffusion coefficients and the corresponding activation energy and to analyze the mechanisms relating to the drying process.

Material and Methods

Experimental device

The dryer presented in this work, is made based on previous work and climatic conditions of the drying environment. This is an indirect solar dryer (1520 x 900 x 550 mm^3) intended for drying fruits and vegetables. The device used, is shown schematically in figure 1. It includes :a solar collector (150 x 1600 x 900 mm3) which is made up of an insulating box having two air circulation holes (inlet and outlet); a 0.5 mm thick galvanized sheet (absorber) painted matte black covering the insulation; a pane (glazing: 5×870×1580 mm3) of ordinary glass covering everything 100 mm above the undulating sheet metal. The air circulates between the window and the absorber. It is first sucked in using three fans placed upstream. The air-absorber contact as well as the convective effect serve to increase the temperature of the drying air. The hot air at the outlet of the solar collector is collected through an air suction pipe to finally reach the in let at the bottom of the drying chamber. The solar 'dryer-collector' system is inclined at an angle of 18.5° to the horizontal, an angle at which the drying temperature must not exceed 60°C in order to avoid deterioration of the dried leaves.

A drying chamber with a rectangular section (800 x 350 x mm2) with a capacity of around 20 kg contains four identical racks (1360x430 x mm2) equidistant by 250mm. Each screen representing a sieve, is made up of a wooden frame to which a very fine mesh nylon mesh is attached. On its upper side, a double-leaf glass door (1360 x 430 x mm2) allows the loading and unloading of products. By passing through the racks, the air comes into contact with the product and takes on the humidity contained there in and is then evacuated to the outside through humid air exhaust openings.

A rectangular wooden support (900×1500×25 mm3) constitutes the main structure of the dryer. This support is carried by four casters allowing easier movement of the device and orientation of the solar sensor according to the position of the sun.

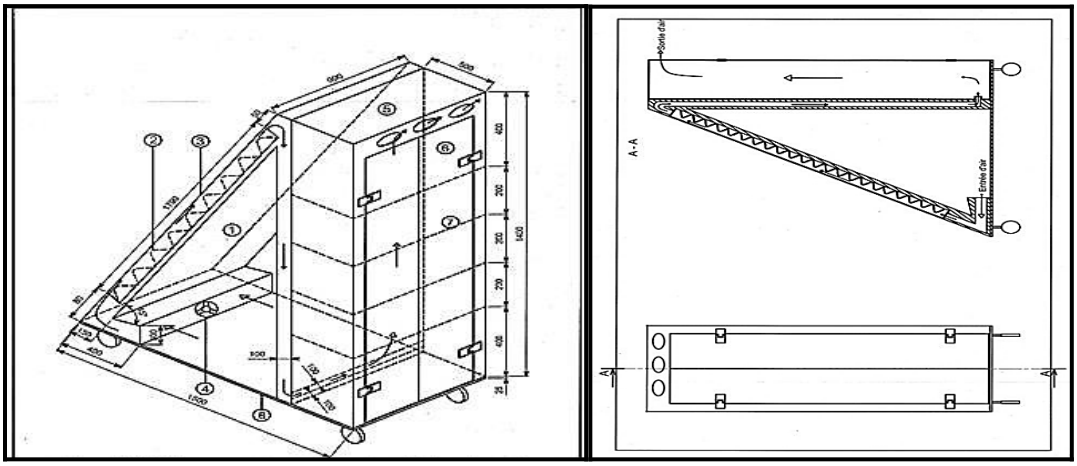

Legend

8	***1***	***support***	***woodwind***	***-***
7	***4***	***rack***	***Stainless steel***	***-***
6	***2***	***door***	***steel***	***-***
5	***1***	***drying box***	***woodwind***	***-***
4	***1***	***ventilator***	***steel***	***-***
3	***1***	***window***	***ordinary glass***	***-***
2	***1***	***absorber***	***Galvanized sheet***	***-***
1	***1***	***box***	***woodwind***	***-***
REPERE	***N.B***	***DESIGNATION***	***MATTER***	***OBSERVATIONS***

Figure 1: Schematic section of the indirect solar dryer produced (LEMA/EPAC/UAC)

Dryer instrumentation

The measurement campaign was carried out at the EPAC/UAC renewable energy solar garden (latitude: 6°26′54″North and longitude: 2°21′20″East) from August 14 to 31, 2016. During each day temperatures are taken between nine and eighteen hours with intervals of fifteen (15) minutes. Six (06) type thermocouples (Testo 635-2) with a diameter of 1mm and a precision of ± 0.5°C were placed throughout the dryer, including one (01) at the entrance to the solar collector and one (01) at its output ; one (01) at the entrance to the drying chamber; one (01) at the level of the rack 3 of the drying chamber, one (01) at the exit of the drying chamber then finally one (01) at the level of the rear part of the solar collector for measuring the ambient temperature. All of the thermocouples are connected to a branded automatic thermometric data recorder (Keithley) with 20 channels and controlled by the Minitab 14 software (fig.2). The temperature measurement interval is 60 seconds. The humidity of the air at the entrance and exit of the box as well as at the levels of the racks are measured using a hygrometric probe with a branded digital display (Humicolor) with a sensitivity of 0.1°C. The air flow is controlled by three fans with the following characteristics: 1300/1550 rpm; 0.2A; 30/5W; 220V; 50/60 Hz and imposes an average speed of 1.6 m/s.

Figure 2 : Instrumentalized indirect solar dryer for temperature measurements.

Water content and drying characteristic curve

The *Moringa oleifera* leaves used in this study are directly picked in their ripe state from plants at least six months old on a moringa production farm in Abomey-Calavi. For each experiment, the leaves are treated and spread in thin layers on each of four (4) mesh racks after half an hour of operation of the drying system. The fresh mass on each rack was around 0.25kg; 0.5kg and 1kg for the different tests. The variation of the wet mass of the product Mh (t) as a function of time, is determined by making static weighing using a precision balance ±0.001g linked to a CD11 model indicator. The time step varies from 10 min at the start of the tests to 30min towards the end of the experiment. The different mass measurements carried out for different drying days allow at the end of the process to establish the drying kinetics once the mass of dry matter is known. The dry mass of the sample is then calculated and that of the quantity of dry product on each rack is deduced by extrapolation. The drying curves are obtained from measurements of the variation in mass of the product over time. The experimental curves X (t)= f(t) are those which contain the most information. The instantaneous water content X (t) of the product is given by the correlation [Eq.1.1] :

$$X(t)(\%) = \left[\frac{m(t)(1+X_o)}{m_o} - 1\right] \boldsymbol{x}\ 100 \quad \text{et } X_0(\%) = \left(\frac{m_e}{m_s} - 1\right) \times 100 \qquad (1.1)$$

The set of curves which represent the variations of the average water content and the drying speed -dX/dt as a function of time (t) then their reduced forms aiming to give a unique representation for the different drying conditions, form the drying kinetics whose reduced forms are given by the following expressions:

$$\phi = \left(\frac{X - X_{eq}}{X_{cr} - X_{eq}}\right) = f(t) \quad (1.2)$$

$$V_r = \frac{V}{V_o} = f\left(\frac{X - X_{eq}}{X_{cr} - X_{eq}}\right) = \left(\frac{X - X_{eq}}{X_{cr} - X_{eq}}\right)^n \qquad (1.3)$$

$$n_t = \left(\frac{\ln V_r}{\ln \varnothing}\right)_t \quad \text{et } n = \sum_i^p n_t \quad (1.4)$$

The theoretical reconstruction of the drying curves requires the determination of the initial water content Xcr and the initial drying speed V_0. Numerous research works agree to affirm that the drying of agri-food products does not present a constant speed phase, that is to say V_0, so it is useful to consider any speed at the start of drying called

speed of drying (Rapusas and Driscoll, 1995). Likewise, Ahouannou (2001) concludes that the initial water content can be assimilated to the critical water content (Xcr = X_0) in the case of agricultural products.
According to Dissa et al. (2016) the drying speed in terms of mass flux density was estimated from the rate of variation of the mass of the product as a function of the drying time according to the relationship [Eq.1.5] :

$$\varphi_m = \frac{-1}{s}\frac{\Delta m}{\Delta t} = \frac{-m_s}{s}\frac{\Delta X}{\Delta t} \approx \frac{m_s}{s}\frac{X(t)-X(t-\Delta t)}{\Delta t} = \frac{m_s}{s}\frac{X(n)-X(n+1)}{\Delta t} \quad (1.5)$$

Where quote is the mass flow (kg water /S.m²) per unit of product exchange surface; t, drying time; Δt, time step between two successive measurements taking place at times n and n+1; X(n) and X (n+1), water contents of the sample estimated at these times and s, exchange surface of the sample.
Finally, the equilibrium water content and the water activity were estimated from each other using the expressions for the desorption isotherm given by the equations [Eq.1.6; 1.7] :

$$X_{eq} = \frac{1}{100}\left[\frac{-ln(1-a_w)}{2{,}33\ X\ 10^{-4}\ (1{,}8\ T_1 + 492)}\right]^{10/7} \quad (1.6)$$

$$a_w = 1 - exp\left[-2{,}33\ X\ 10^{-2{,}6}\ (1{,}8\ T_1 + 492) X_{eq}{}^{0{,}7}\right] \quad (1.7)$$

Where Xeq is the equilibrium water content, T1 is the air temperature in hygroscopic equilibrium with the product and aw is the water activity.

Modeling drying curves
The five models used in this work are nonlinear models (Table 1).

Table 1 : Mathematical models used

Modèles	Equation
Verma and al. (1985)	$X^* = aexp(-kt) + (1-a)exp\ (-gt)$
Approximation of diffusion (1998)	$X^* = aexp(-kt) + (1-a)exp\ (-kbt)$
Logarithmic (1999)	$X^* = aexp(-kt) + c$
Henderson and Pabis modified (1999)	$X^* = aexp(-kt) + bexp(-gt) + cexp(-ht)$
Midilli and al. (2002)	$X^* = a\ exp(-kt^n) + bt$

The first three models, namely the model of Verma and al. (1985), the diffusion approximation (1998) and the logarithmic model (1999) depend on three parameters. The modified Henderson and Pabis model (1999) depends on five parameters. The model of Midilli and al. (2002) depends on four parameters. All these parameters are calculated using the Levenberg-Marquardt algorithm. Scilab software was used to calculate the coefficients.

Principle of the Levenberg-Marquardt algorithm
Before stating the principle of the Levenberg-Marquardt algorithm, we will give the following definitions.
Definition1. Let A € Mn (R) be the set of square matrices of size n.

$$If\ A = \begin{pmatrix} a_{11} & a_{12} & \dots & a_{1n} \\ a_{21} & a_{22} & \dots & a_{2n} \\ \vdots & \vdots & \ddots & \vdots \\ a_{n1} & a_{n2} & \dots & a_{nn} \end{pmatrix}$$

$$then\ diag(A) = \begin{pmatrix} a_{11} \\ a_{22} \\ \vdots \\ a_{nn} \end{pmatrix}$$

Definition2. Let be f : $(x_1, x_2, \dots, xn) \in R^n \rightarrow f(x_1, x_2, \dots, xn) \in R$.
The Jacobian matrix of f is given by :

$$J = \begin{pmatrix} \frac{\partial f}{\partial x_1} & \frac{\partial f}{\partial x_2} & \frac{\partial f}{\partial x_3} \dots \frac{\partial f}{\partial x_n} \end{pmatrix}$$

The transpose of J denoted J^T is given by :

$$J^T = \begin{pmatrix} \frac{\partial f}{\partial x_1} \\ \frac{\partial f}{\partial x_2} \\ \frac{\partial f}{\partial x_3} \\ \vdots \\ \frac{\partial f}{\partial x_n} \end{pmatrix}$$

The Levenberg–Marquardt algorithm (LMA), is used to solve non-linear least squares problems (K. Madsen and al., 2004; Aude Rondepierre and al., 2018 ; Henri P.Gavin and al., 2020 ; Ananth Ranganathan and al., 2004 ; Marius Kaltenbach, 2022). This algorithm was first published by Kenneth Levenberg (Kenneth Levenberg, 1944) while working at the Frankford Army Arsenal in USA. It was rediscovered by Donald Marquardt (Marquardt Donald, 1963) who worked as a statistician at DuPont, an american multinational chemical company. The primary application of the Levenberg–Marquardt algorithm is in the least-squares curve fitting problem : given a set of n empirical pairs (xi, yi) of independent and dependent variables,1find the parameters β of the model curve f(x, β) so that the sum of the squares of the deviations S(β) is minimized (K. Madsen and al., 2004 ; Aude Rondepierre and al., 2018 ; Henri P.Gavin and al., 2020 ; Ananth Ranganathan and al., 2004 ; Marius Kaltenbach, 2022) :

$$S(\beta) = \sum_{i=1}^{n} \left(y_i - f(x_i, \beta)\right)^2$$

The Levenberg–Marquardt algorithm is an iterative procedure. To start a minimization, the user has to provide an initial guess for the parameter vector β. In cases with only one minimum, an uninformed standard guess like β = (1, 1, . . . , 1) will work fine. In each iteration step, the parameter vector β is replaced by a new estimate β+δ. To determine δ, the function f (xi, β + δ) is approximated by its linearization:

$$f(x_i, \beta + \delta) = f(x_i, \beta) + J_i\delta_i$$

Where $J_i = \frac{\partial f(x_i,\beta)}{\partial \beta}$ is the gradient of f, with respect to β.

After calculations, we get :

$$\delta = [(J^T J) + \lambda diag(J^T J)]^{-1}.J^T.(y - f(\beta))$$

where J is the Jacobian matrix, whose i-th row equals Ji and f(β) and y are vectors with i-th component f(xi, β) and yi respectively, λ is a real parameter, J^T is the transpose of the Jacobian matrix, J^T J is a n × n square matrix. The LMA takes the form :

1. β_0 is the initial value.
2. $\beta_n = [JT\ J + \lambda\ diag\ (JT\ J)]^{-1}.J^T\ .(y - f(\beta))$.
3. $\beta_0 = \beta_0 + \beta_n$ update (Samir KENOUCHE, 2018)
4. Stop criterion

The best model is selected according to the following criteria: • High correlation coefficient (r) • Minimum mean systematic error (MSE) • Minimum reduced χ squared. These statistical parameters are calculated as follows :

$$r^2 = \sqrt{\frac{\sum_{i=1}^{n}(X^*_{pre} - \overline{X^*_{exp}})^2}{\sum_{i=1}^{n}(X^*_{exp} - X^*_{exp})^2}} \qquad (1.8)$$

$$\chi^2 = \sqrt{\frac{\sum_{i=1}^{n}(X^*_{exp} - X^*_{pre})^2}{N - n}} \qquad (1.9)$$

$$ESM = \frac{100}{N}\sum_{i=1}^{N}\left|\frac{X^*_{exp} - X^*_{pre}}{X^*_{exp}}\right| \qquad (1.10)$$

Results and Discussions:-

Evolution of temperature and relative humidity of the air during drying

Figures 3 (a,b) respectively illustrate the evolutions of drying (Ts) and ambient (Tamb) temperatures as a function of drying time. The curves provided have almost similar appearances and the fluctuating temperature profiles observed are a function of the time of day, the drying air flow and the mass of the product to be dried. These variations demonstrate a satisfactory agreement with temperature maxima around 55°C between noon and fourteen hours and minima around 38°C at low solar radiation. We note that a high mass of the product to be dried slows down the evolution of the temperature of the drying air in the cabinet with a longer drying time. Indeed, the continuous extraction of water vapor from the product contributes significantly to thermal mass exchanges and increases the hygrometric power of the drying air which, upon leaving the dryer, becomes more humid. Figures 4(a, b) confirm these facts where the curves of the relative humidity of the drying air show an evolution inversely proportional to that of the temperature of the ambient air. Humidity has high values during the period of low solar radiation and low values during the sunny period, thus favoring the drying process.

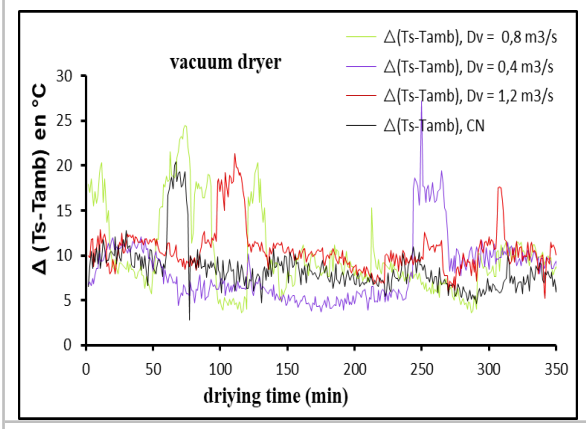
vacuum dryer
△(Ts-Tamb), Dv = 0,8 m3/s
△(Ts-Tamb), Dv = 0,4 m3/s
△(Ts-Tamb), Dv = 1,2 m3/s
△(Ts-Tamb), CN
Δ (Ts-Tamb) en °C
driying time (min)

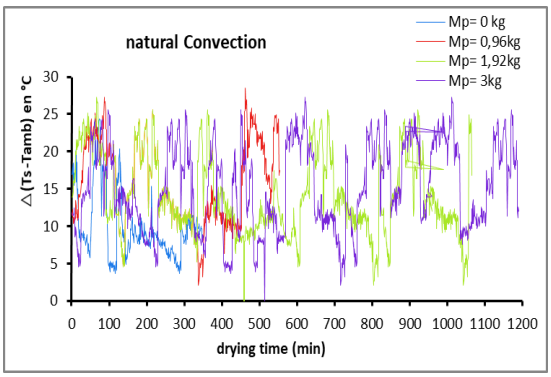
natural Convection
Mp= 0 kg
Mp= 0,96kg
Mp= 1,92kg
Mp= 3kg
△(Ts-Tamb) en °C
drying time (min)

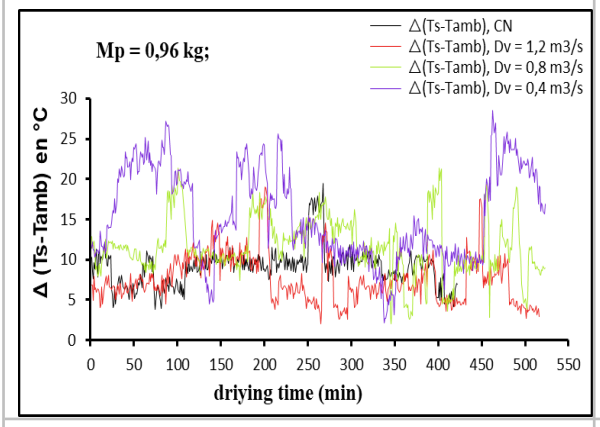
Mp = 0,96 kg;
△(Ts-Tamb), CN
△(Ts-Tamb), Dv = 1,2 m3/s
△(Ts-Tamb), Dv = 0,8 m3/s
△(Ts-Tamb), Dv = 0,4 m3/s
Δ (Ts-Tamb) en °C
driying time (min)

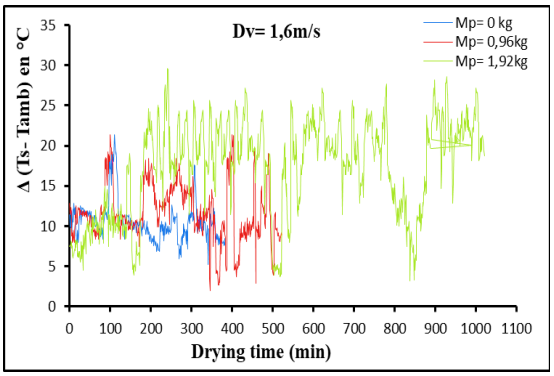
Dv= 1,6m/s
Mp= 0 kg
Mp= 0,96kg
Mp= 1,92kg
Δ (Ts- Tamb) en °C
Drying time (min)

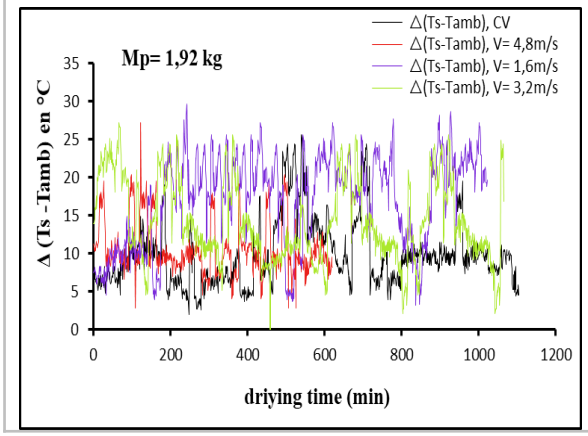
Mp= 1,92 kg
△(Ts-Tamb), CV
△(Ts-Tamb), V= 4,8m/s
△(Ts-Tamb), V= 1,6m/s
△(Ts-Tamb), V= 3,2m/s
Δ (Ts -Tamb) en °C
driying time (min)

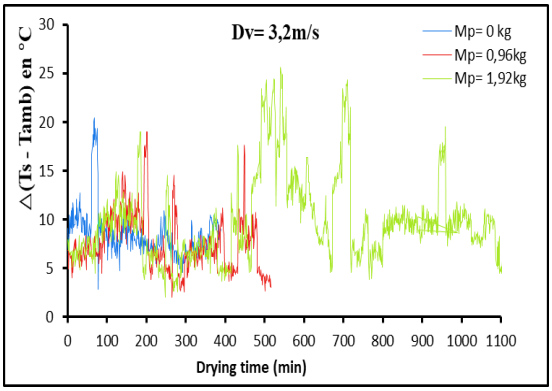
Dv= 3,2m/s
Mp= 0 kg
Mp= 0,96kg
Mp= 1,92kg
△(Ts - Tamb) en °C
Drying time (min)

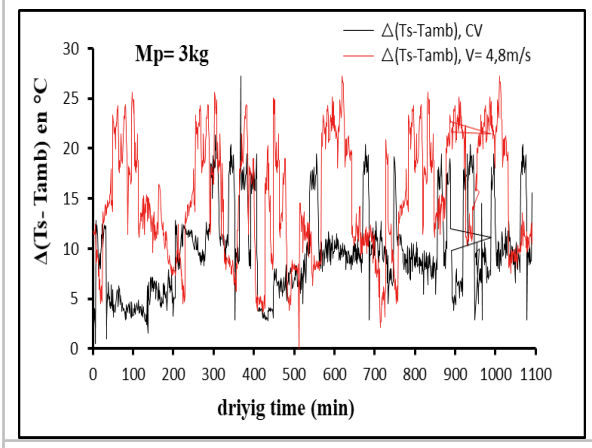

Figure 3a : Difference between ambient temperature (Tamb) and drying temperature (Ts) as a function of drying time and mass for different air speeds

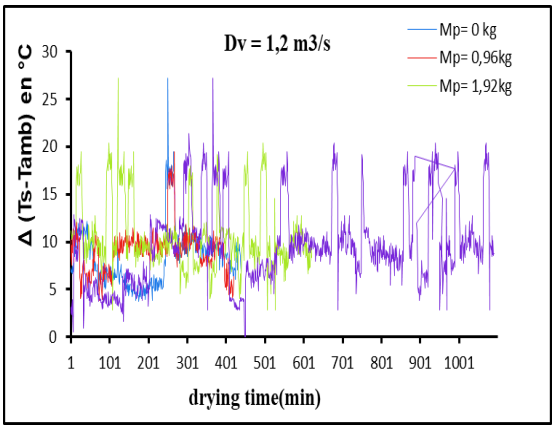

Figure 3b : Difference between ambient temperature (Tamb) and drying temperature (Ts) as a function of drying time and air speed for different mass of product

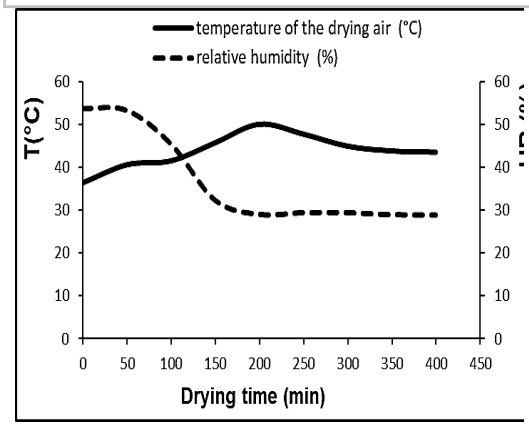

Figure 4a : Evolution of air humidity and temperature inside the dryer

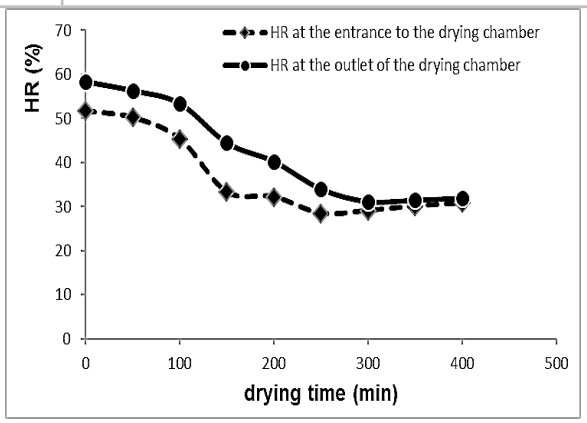

Figure 4b : Relative humidity (HR) of the air as a function of drying time

Kinetics of convective drying of Moringa oleifera leaves

Influence of drying air temperature

The drying kinetics obtained for different drying air conditions are presented in figure 5. Note that for the same drying air flow rate, an increase in temperature leads to a reduction in drying time and water content of the product by offering a greater water vapor pressure deficit, one of the driving forces in the process of diffusion of humidity towards the exterior. Indeed, the increase in drying potential and reduction in drying time is explained by the fact that the rise in temperature leads to an increase in the intensity of heat transfer and accelerates the migration of water to the inside the product. For the same drying air temperature, an increase in the drying air flow promotes acceleration of the drying process by involving convective exchanges. Experimentally, for a temperature of 50°C and an air flow rate of 1.2 m3/s, it takes approximately 450 min to dry 1kg of leaves to a water content of 0.112 g water/gms. A decrease in temperature of 5°C increases the drying time by 145 min to reach this same content (fig.5a, b)

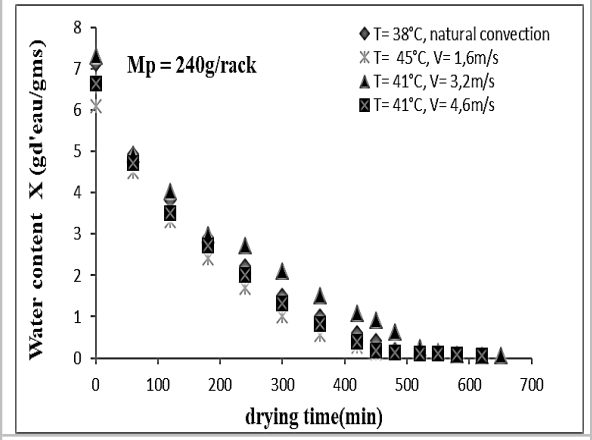

Figure 5a : Water content as a function of drying time

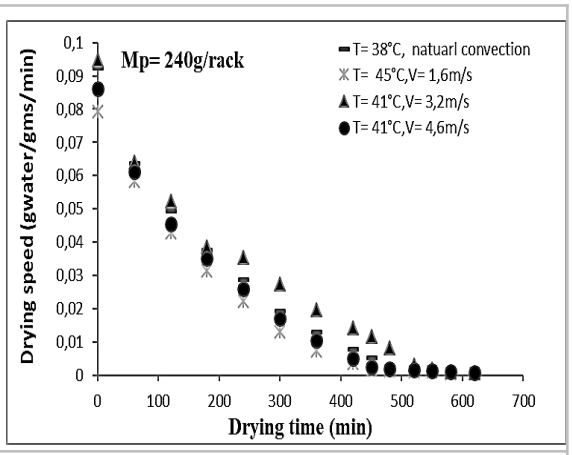

Figure 5b : Drying speed as a function of drying time

Influence of drying air speed

The curves representing the influence of air flow (fig.6a) and temperature (fig.6b) on the drying speed show the absence of periods of product heating (phase 0) and drying at constant speed (phase 1). Only the period with a decreasing rate (phase 2) is present. This observation is explained by the absence of free water on the surface of the product and also in the structure of the latter. These results are in agreement with those published in the literature for different plant products (Moctar, 2024; Mariem and Mabrouk, 2017; Koua et al., 2017). Indeed, Bimbenet et al. (1984) reported that the heating period practically disappears when the product is in particles or sheets and that the constant rate period is not observed in many cases when it comes to plant products. Drying during the decreasing rate phase is essentially governed by the diffusion of water in the solid. It is a complex mechanism involving water in both liquid and vapor states, which is often characterized by effective diffusion. In fact, increasing the temperature of the drying air generally causes an increase in the drying speed, particularly at the start of the drying operation. However, towards the end of the operation the influence of this parameter is weak. This is explained by the fact that almost all of the free and bound water molecules have been evaporated and only the water molecules linked to the structure of the product remain which are not affected by the drying operation.

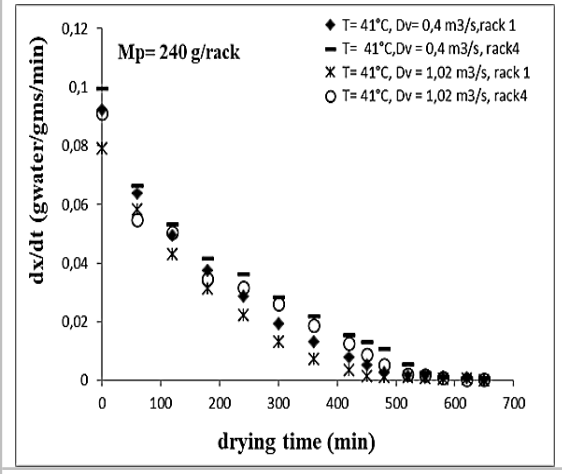

Figure 6a: Influence of air flow on drying speed_

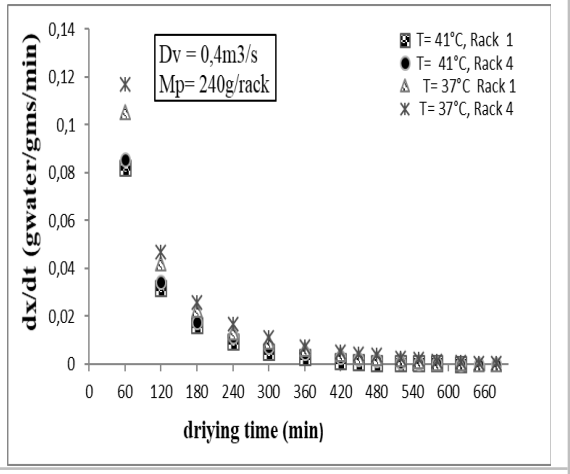

Figure 6b**:** Influence of temperature on drying speed

Figure7a provides a unique representation of the drying kinetics of Moringa oleifera leaves. A perfect grouping of the cloud of experimental points, observed at different temperatures and drying air flow rates, shows that there exists a value of "n" for which all the experimental curves could be replaced by a single curve representative of the form Φn, with n=1.75.

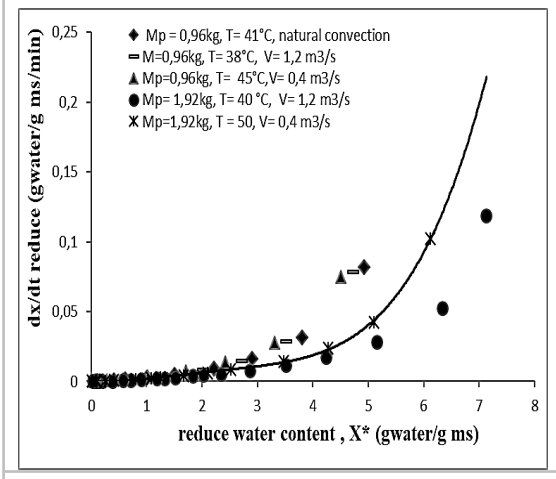

Figure7a : Drying Characteristic Curve (CCS) of *M. oleifera* leaves

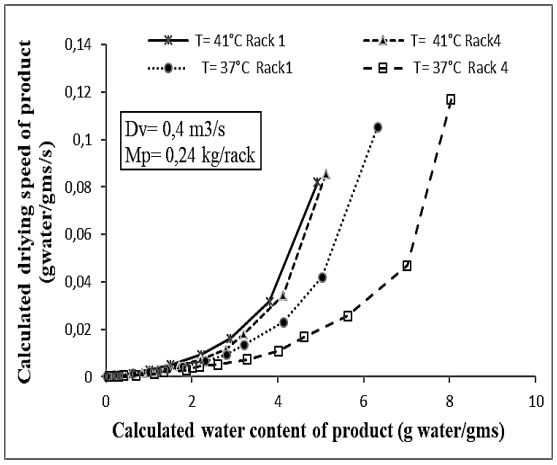

Figure7b : Drying speed as a function of water content

Smoothing the Drying Characteristic Curve (CCS) made it possible to determine the characteristic equation of the drying speed in the form of a polynomial of degree 4 :

$$f\left(\frac{-\frac{dX}{dt}}{\frac{dX}{dt}}\right)_{in} =$$ 0, 0003X*^{4}- 0, 0023 X*^{3}- 0, 0065 X*^{2}-0,0033X* + 0,0005 ;

QUOTE

r^2= 0, 9994 ; ESM = 0, 94753834457320

No linear regression driven by Minitab14 software was used and the correlation coefficients of each model were determined. For these models, the R^2 ranged from 0.9612 to 1 and the ESM from 2.45612 10^{-6} to 3.5673 10^{-3} (Table 2). The model of Midilli and al. (2002) has the highest R^2 (R^2=1) and the lowest ESM (ESM=2.45612 10^{-6}) with good simulation of the experimental points (Fig.8a and 8b). For each of the simulated water content curves, we see that the water content hardly changes beyond 450 min and is of the order of 0.113 g water/gms (11.3% bs). The hygroscopic equilibrium of the product is there fore reached at the end of this drying time.

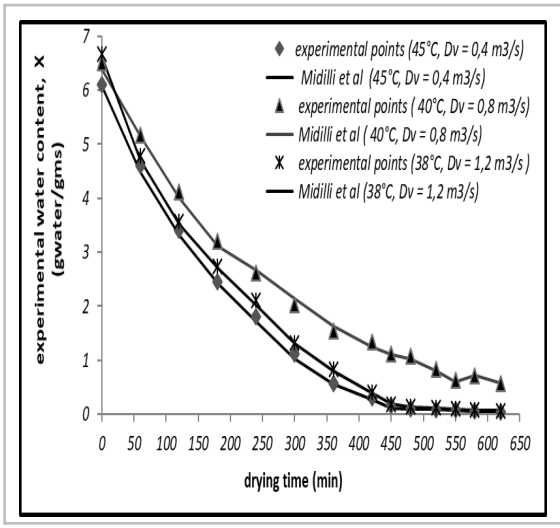

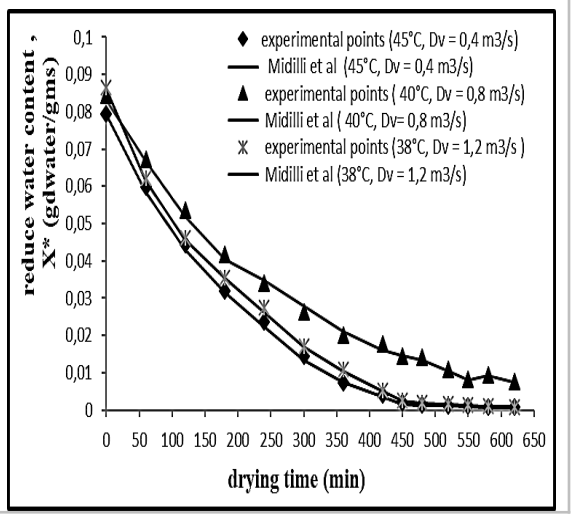

Figure 8a: Experimental and predicted curves	Figure 8b:Reduced and predicted curves

Table 2 : Values of estimated parameters and criteria for statistical choice of the model

Models	Dv (m^3/s)	T (°C)	Coefficients	r^2	χ^2	RMSE
Verma and al. (1985)	0,4	40	K = 0,0132; a = 0,0470; g = 0,96452	0,9866	$9,6553\ 10^{-4}$	0,02557
		45	K= 0,0143; a = 0,0481; g = 0,00678	0,9867	$10,436\ 10^{-4}$	0,01969
		50	K= 0,0156; a = 0,0499; g = 0,02342	0,9875	$10,756\ 10^{-4}$	0,00502
Approximation of diffusion (1998)	0,4	40	K= 0,03076; a = 1,077; b = 1,0021	0,9867	$9,2248\ 10^{-4}$	0,03164
		45	K=0,03076; a = 1,0877; b = 0,0231	0,9721	$9,2248\ 10^{-4}$	0,01417
		50	K=0,03076; a = 1,0887; b = 0,9876	0,9776	$9,2248\ 10^{-4}$	0,02216
Logarithmic (1999)	0,4	40	K= 0,008; a = 1,01242; c = - 0,14532	0,9908	$3,5673\ 10^{-3}$	0,01969
		45	K= 0,008; a = 1,03842; c = - 0,14632	0,9914	$4,4574\ 10^{-3}$	0,02040
		50	K= 0,008; a = 1,04742; c = - 0,21532	0,9801	$6,7879\ 10^{-3}$	0,02557
Henderson and Pabis modified (1999)	0,4	40	a=-0,009; b= $1,64\ 10^{-5}$; k = 0,0136; g= 1,0021; h = 0,0534	0,9866	$3,014310^{-3}$	0,01417
		45	A=-0,0127; b= $1,610^{-5}$; k= 0,0124; g= 0,99874; h= 0,54671	0,9889	$3,011\ 10^{-3}$	0,02452
		50	a = - 0,0134; b = $1,610^{-5}$; k= 0,0178; g= 0,2324; h = 0,00987	0,9867	$3,022\ 10^{-3}$	0,02040
Midilli and al(2002)	0,4	40	a = 0,9231; k = 0,0097; n = 0,9878; b = $3,19\ 10^{-4}$	1	$2,4562\ 10^{-6}$	0,00606
		45	a = 0,9791; k = 0,017; n = 0,9878; b= $3,20\ 10^{-4}$	1	$2,1112\ 10^{-6}$	0,00435
		50	a = 0,9266; k = 0,0219; n = 0,9878; b= $3,10\ 10^{-4}$	0,9999	$3,2312\ 10^{-6}$	0,00210

Influence of the position of the racks on the loss of mass of the product during drying

We followed the evolution of the weight loss of the product as a function of the drying time and following the position of the racks in the dryer for different drying air and mass conditions (fig.9). At each moment of drying we see that the water content varies with the position of the racks in the direction of the air flow. Rack 1 placed at the bottom of the unit where the air is warmer shows the lowest water contents while rack 4 located at the top has the highest water contents. This observation was made by Dissa et al. (2009 ; 2016) respectively for the solar drying of mango and spirulina. In fact, when moving from a lower rack to a higher rack, the air temperature drops and its hygrometric rate increases. This causes an increase in the water vapor pressure in the air and a reduction in the exchange potential which is defined by the difference between the vapor pressure at the surface of the product and the water vapor pressure in the air.

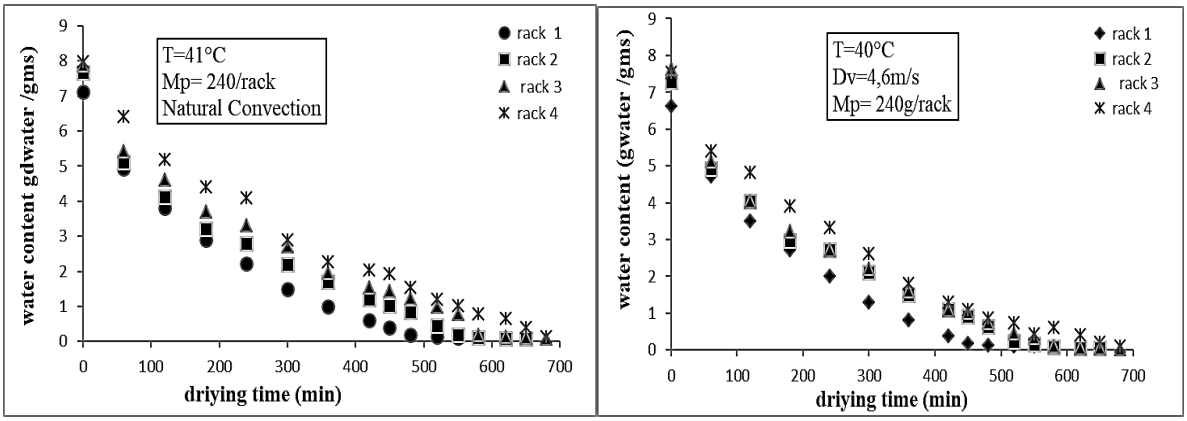

Figure 9 : Influence of the position of the racks on the weight loss of the product during drying

Effective diffusion and activation energy

Material transfer during drying is controlled by internal diffusion. Fick's second law of diffusion, shown in equation (1.12), has been widely used to describe the drying process for most organic products (Srikiatden et al., 2008).

$$\frac{\partial X}{\partial t} = D_{eff}\frac{\partial^2 X}{\partial x^2} \qquad (1.12)$$

X = water content (water/gms) ; t= time (s) ; x = sample thickness (m) ; Deff = diffusion coefficient (m2/s). The analytical solution of this Fick law developed by Crank (1975) can be expressed by (Eq1.13) :

$$X^{*} = \frac{X(t)-X}{X_0-X} = \frac{8}{\pi^2}\sum_{n\approx 0}^{\infty}\frac{1}{(2n+1)^2}\exp\left[-(2n+1)^2\frac{\pi^2 D_{eff}}{4L^2}\right] \qquad (1.13)$$

When the time issufficiently long, all the terms of the series are negligible compared to the first and we obtain :
Where L (m) is the thickness of the Moringa oleifera leaf.
Deff values are usually determined by the graphical method by plotting experimental drying data in terms of ln X* versus drying time (t) (fig.10).

The result is a slope line ($\pi^2 D_{eff}$ /$4L^2$) that can be used to calculate the effective diffusion coefficient for different aerothermal conditions (Table 3).

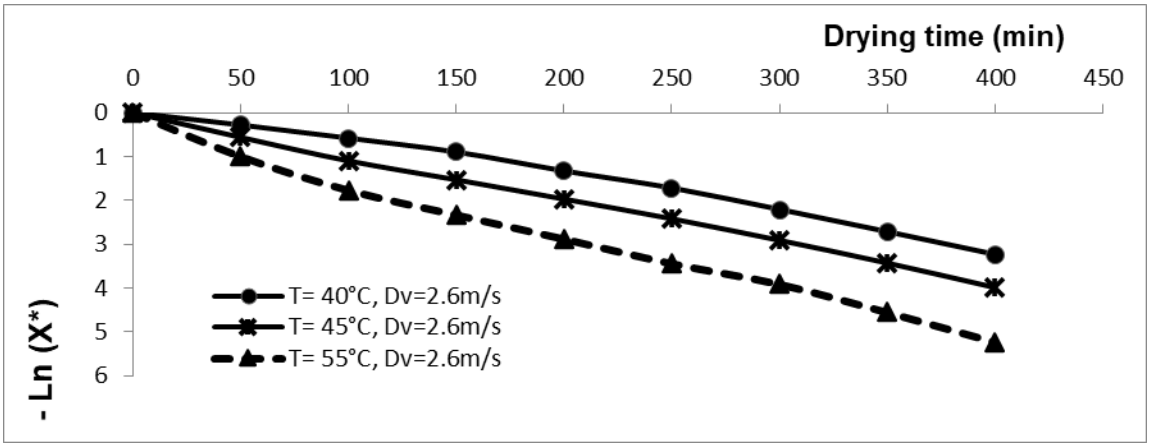

Figure 10 : Simultaneous effects of temperature and air flow on the effective diffusion coefficient of M. oleifera leaves

Table 3 : Deff values for M. oleifera leaf

Dv (m^3/s)	T (°C)	Deff ($m^2.s^{-1}$)	R^2	Ea ($KJ.mol^{-1}$)	D_o (m^2s^{-1})
0,4	**38**	$8,456\ 10^{-11}$	0,9912	86,46223	0,0687646
	45	$5,856\ 10^{-10}$	0,9867		
	50	$9,9237\ 10^{-10}$	0,9634		
0,8	**37**	$5,231\ 10^{-10}$	0,9968	89,2341	0,07896
	40	$7,1928\ 10^{-9}$	0,9869		
1,2	**38**	$9,8965\ 10^{-10}$	0,9868	91,2125	0,08231
	41	$3,8765\ 10^{-9}$	0,9998		
	43	$8,9567\ 10^{-8}$	0,9999		

The analysis of table 3 reveals that the effective diffusivity Deff increases with temperature and drying air flow. In our case, these values vary from $8.456\ 10^{-11}$ to $8.9567\ 10^{-8}$ (m^2s^{-1}) and are indeed in the range of 10^{-12} - 10^{-8} (m^2s^{-1}), relating to the products agro-food industries (Lahmari et al., 2012 ; Mariem and Mabrouk 2017 ; Koua et al., 2017). The origin of self-diffusion is thermal agitation. Diffusion is there fore thermally activated, and the diffusion coefficient follows an Arrhenius law (Lahmari et al., 2012) :

$$D_{eff} = D_0\, exp\left[-\frac{E_a}{RT}\right] \qquad (1.15)$$

Equation (1.15) can be rearranged in to the form :

$$Ln\,(D_{eff}) = Ln(D_0) - \frac{E_a}{R}\left(\frac{1}{T}\right) \qquad (1.16)$$

The activation energy is calculated by representing the natural logarithm of the experimental values of the effective diffusivity D_{eff} as a function of the reciprocal of the temperature (Fig.13). It is a straight line which indicates the dependence of Arrhenius in the range of temperatures studied. This dependence can be represented by equation (Eq1.17), which represents the influence of the temperature of the drying air on the effective diffusivity.

$$D_{eff} = 0{,}0687646\ exp\left(\frac{-10.398992}{T}\right) (1.17)$$

From the slope of the line described by equation (1.17) and shown in Figure 11, we derive an activation energy Ea = 86.46223 (KJ.mol-1) with a correlation coefficient r = 0.9912 for an air flow Dv = 0.4m3/s and 38°C < T < 50°C (table 3).

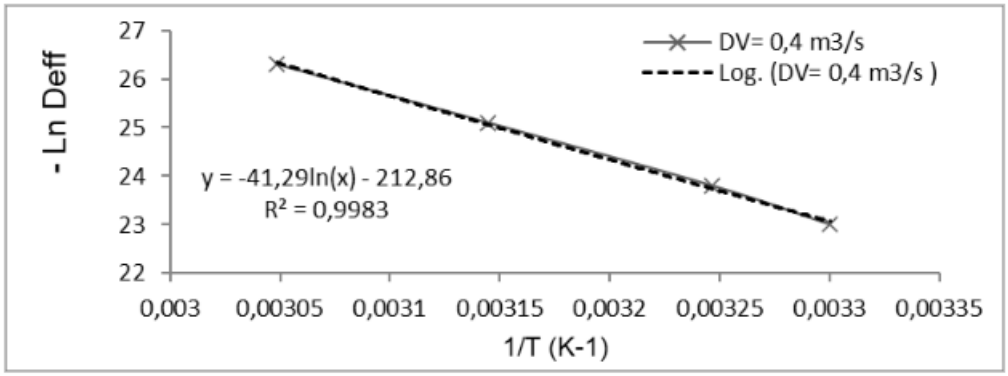

Figure 11 : Influence of drying air temperature on the effective diffusion coefficient of M. oleifera leaves

Conclusion:-

The theoretical and experimental study undertaken on the drying of agricultural products at the Applied Energy and Mechanics Laboratory (LEMA) of the Ecole Polytechnique d´Abomey-Calavi consisted on the one hand of the creation of an indirect solar dryer and the evaluation of its thermal performances and on the other hand the study of the kinetics of convective drying and thermal hydric diffusivity of the leaves of Moringa oleifera (Lam). The experimental results made it possible to assess throughout the test period the thermal efficiency of the dryer which has maximum temperatures around 55°C in strong solar radiation and minimums around 38°C. The presence of a single phase with decreasing speed was noted. Temperature, air speed and radiation intensity are the most influential parameters on the solar drying operation. The Drying Characteristic Curve is obtained and the drying rate equation is determined empirically. The effective diffusivity Deff increases with temperature and hot air flow. The activation energy is determined using the Arrhenius equation. A supplement could considerably reduce the drying time, with elimination of down time during periods of low insolation. It would be important to test our dryer prototype throughout the year to make necessary modifications and adjustments to improve its efficiency.

Conflict of Interest Statement

The authors declare no conflicts of interest associated with this manuscript.

References:-

1. Ahouannou Clément, Goudjinou Codjo, Osséni G. Sibiath, Adounkpe Julien, HounkpatinWaliouAmoussa, Kounouhewa Basile (2023) : Estimation of ThermodynamicParameters for Better Conservation of FreshTomato (Lycopersicumesculentum) ; Advances in Chemical Engineering and Science, 13, 149-171
2. Ahouannou, C (2001). Etude du séchage de produits agroalimentaires tropicaux : application au manioc, gingembre, gombo et piment. Thèse de doctorat, Université Nationale du Bénin, spécialité : Energétique, C.P.U/ FAST, N° d'ordre : 08, 219p.
3. Ananth Ranganathan, The Levenberg-Marquardt Algorithm, Juin 2004
4. Aude Ronde pierre, méthodes numériques pour l'optimisation non linéaire déterministe, Département Génie Mathématique et Modélisation, 2018.
5. Bimbenet J.J (1984). 'Le Séchage dans les Industries Agricoles et Alimentaires', Les Cahiers du Génie Industriel Alimentaire (GIA), Edité par la Sepaic, Paris, 2ème Edition, p. 34.

6. Boubekri A, Benmoussa H, Mennouche D (2009). Solar Drying Kinetics of Date Palm Fruits Assuming a step-wise air temperature change, Journal of Engineering science and Technology, 4 (3) : 308-320
7. Brito thibauthéon Arron Sonagnon, Aboudou Kowiou, Goudjinou Codjo, Alidou chérif, Zannou aimé, Gbaguidi magloire et Soumanou Mohamed Mansourou (2021). Qualités physico-chimique et microbiologique de deux espèces de poissons importés (trachurus trachurus et scomber scombrus) et locaux (clarias garieprinus et oreochromis aureus) commercialisés au bénin urbain ; rev. Ivoir. Sci. Technol., 38 : 311 – 323.
8. Dissa A O, Tiendrebeogo E, Garba S, Koulidiati J (2016). Modélisation et simulation du séchage solaire en couche mince de la Spiruline (Asthrospiraplatensis, Journal de la Société Ouest-Africaine de Chimie, 042 : 1–721ème Année, Décembre 2016.
9. Dissa AO, Bathiebo J, Kam S, Savadogo PW, Desmorieux H, Koulidiati J (2009). Modelling and experimental validation of thin layer solar drying of mango slices. Renewable Energy, 34: 100-1008.
10. Goudjinou C (2018) : ‘’Etude théorique et expérimentale du séchage solaire des feuilles de Moringa oleifera (Lam) : Etat des lieux,caractérisation thermophysique, physico-chimique et fonctionnelle de la poudre dérivée’’.
11. Goudjinou C, Ahouannou C, Chaffa G, Soumanou MM (2017).Thermophysical characterization of the powder resulting from the solar drying of the Moringa oleifera leaves. International Journal of Engineering, Science and Technology, 9 (4): 28-47
12. Henri P. Gavin, The Levenberg-Marquardt algorithm for nonlinear least squares curve-fitting problems, Department of Civil and Environmental Engineering Duke University, septembre 2020
13. K. Madsen, H.B. Nielsen, O. Tingleff, METHODS FOR NONLINEAR LEAST SQUARES PROBLEMS, Avril 2004
14. Koua K, Magloire EP, Gbaha P (2018). Séchage des fèves de cacao dans un séchoir solaire indirectà circulation forcée d’air, Revue du CAMES- Sciences Appliquées et de l’IngénieurCames 2017, 2(2) : 15-19.
15. Koua K, Magloire EP, Gbaha P (2018). Séchage des fèves de cacao dans un séchoir solaire indirectà circulation forcée d’air, Revue du CAMES- Sciences Appliquées et de l’IngénieurCames 2017, 2(2) : 15-19.
16. Lahmari N, Fahloul D, Azani I (2012). Influence des méthodes de séchage sur la qualité des tomates séchées (variété Zahra). Revue des Energies Renouvelables; 15 (2) 285-295.
17. Levenberg Kenneth, A Method for the Solution of Certain Non-Linear Problems in Least Squares,Quarterly of Applied Mathematics, 1944.
18. Mariem S B, Mabrouk S B (2017). Cinétique de séchage et Courbe caractéristique de séchage d’une couche mince de tomate 18eme journées internationale de thermiques (JITH 2017), Monastier (tunisie) du 25 – 27 Octobre 2017.
19. Marius Kaltenbach, The Levenberg-Marquardt Method and its Implementation in Python, Master Thesis, Department of Mathematics and Statistics Konstanz, Décembre, 2022
20. Marquardt Donald, An Algorithm for Least-Squares Estimation of Nonlinear Parameters SIAM Journal on Applied Mathematics, 1963.
21. Masmoudi G, Hermassi I, Azzouz S, Belghith A (2008). Caractérisationexpérimentale du raisin sultanine: Cinétique de séchage et rhéologie. Revue des Energies Renouvelables SMSTS’08 Alger 81 (1): 416–335.
22. Midilli A, Kucuk H, Yapar Z (2002). A new model for single layer drying. Drying Technology, 20 (7): 1503-1513.
23. SAMIR KENOUCHE, Algorithmes d’optimisation : application à des fonctions-objectifs non-linéaires, Master Physique, DÉPARTEMENT DES SCIENCES DE LA MATIÈRE-UMKB, MÉTHODES MATHÉMATIQUES ET ALGORITHMES POUR LA PHYSIQUE, 2018
24. Srikiatden J, Roberts JS (2008). ‘Predicting Moisture Profiles In Potato And Carrot During Convective Hot Air Drying Using Isothermally Measured Effective Diffusivity’, Journal of Food Engineering, 84 (4): 516–525.
25. Stephen Campbell, Jean-philippe Chancelier, Ramine Nikoukhah, modeling and simulation in Scilab/Scicos, Springer, 2006.
26. Verma LR (1985). Effects of drying air parameters on rice drying models, Transactions of the American Society of Agricultural Engineers, 28: 296-30.